2023

# INVESTIGATING CHANGES IN ER-TO-GOLGI PROTEIN TRANSPORT FOLLOWING A SHORT CALCIUM PULSE: ROLES OF ALG-2 AND PEFLIN

ALAA MOHAMMED YOSRI SHAHEEN
*University of Montana, Missoula*

# INVESTIGATING CHANGES IN ER-TO-GOLGI PROTEIN TRANSPORT FOLLOWING A SHORT CALCIUM PULSE: ROLES OF ALG-2 AND PEFLIN

By

ALAA MOHAMMED YOSRI SHAHEEN

Bachelor Of Dental Science, Mansoura University, Mansoura, Egypt, 2012

Thesis

presented in partial fulfilment of the requirements
for the degree of

Master of Science
in Cellular, Molecular and Microbial Biology

The University of Montana
Missoula, MT

December 2023

Approved by:

Scott Whittenburg, Dean of The Graduate School
Graduate School

Jesse C. Hay, Research Advisor
Division Of Biological Sciences

Mark Grimes, CMMB Member
Division Of Biological Sciences

Sarah Certel, CMMB Member
Division Of Biological Sciences

Klara Briknarova, Outside Member
Department of Chemistry and Biochemistry

Shaheen, Alaa, M.S., December 2023 Cellular, Molecular and Microbial Biology

Abstract

Chairperson or Co-Chairperson: Jesse C. Hay

Co-Chairperson: N/A

The ER-Golgi interface is a very dynamic environment that involves the movement of protein-loaded vesicles forward and backward. The movement of COPII-coated vesicles from the ER to the Golgi is the initial step in the movement of secreted, organellar, and cell surface proteins toward their final destinations. Many factors can regulate this step, including cytosolic calcium increases. In this study, we examined the effect of a transient calcium pulse on recruitment to ER exit sites of cargo proteins for ER export, the calcium-sensitive regulatory proteins apoptosis-linked gene 2 (ALG-2) and peflin, and the COPII outer coat subunits Sec31A and Sec13. We used immunofluorescence and live cell microscopy in normal rat kidney cells to monitor these events during and after a calcium surge induced by the ER calcium pump inhibitor 2,5-Di-(t-butyl)-1,4-hydroquinone (BHQ). We found that a calcium pulse can enhance the sorting of cargo proteins into ER exit sites for at least one hour following the pulse. This functional enhancement coincided with the recruitment of the outer coat proteins Sec13 and Sec31A to ER exit sites that persisted well beyond the calcium pulse. These functional and targeting changes were most likely directed by the calcium sensors ALG-2 and peflin, whose calcium-dependent kinetic recruitment patterns were also documented. One unexpected finding was that peflin recruitment to ER exit sites was increased by calcium; previous results had suggested that peflin would dissociate in response to calcium. Taken together our work demonstrates for the first time that a brief calcium event can initiate a cascade of functional and structural changes at ER exit sites that persists well beyond the period of elevated calcium. Such calcium-dependent regulation may ensure more efficient protein movement in the early secretory pathway after calcium-induced exocytosis of secretory vesicles or following the induction of cell proliferation or differentiation

# Chapter 1: Introduction

The endoplasmic reticulum is the first organelle in the secretory pathway and the main store for calcium in the cell. It holds about 100 to 1000 μM of free $Ca^{2+}$ in its lumen [1,2]. In contrast, the cytosol contains ≤100 nM of free calcium under resting conditions [3]. This allows the ER to be a major hub for calcium signaling in response to different stimuli. Also, the high calcium concentration inside the ER is essential for proper functioning of the chaperones and oxidases that assist correct protein folding [4]. Calnexin, calreticulin and BiP are major chaperones in the ER and are calcium binding proteins [5,6,7]. ER calcium depletion can impair the folding machinery, causing the accumulation of unfolded and misfolded proteins in the ER which can lead to ER stress [8].

Calcium movement into and out of the ER is controlled by a calcium pump and calcium channels (figure 1). The Sarco-endoplasmic Reticulum Calcium ATPase (SERCA) pump utilizes energy from ATP hydrolysis to pump calcium into the ER lumen [9]. In contrast, the inositol 1,4,5-trisphosphate receptors (IP3Rs) and the Ryanodine receptors (RyRs) are channels that allow calcium release from the ER into the cytosol in response to different activators. The IP3 receptors can be activated by IP3 [10] generated when phospholipase C hydrolyses phosphatidylinositol 4,5-bisphosphate (PIP2). The Ryanodine receptors can be activated by calcium, apo-calmodulin or the adenine nucleotides ATP, ADP and AMP [11]. Once a calcium signal is produced in the cytosol, it's rapidly cleared by the SERCA pump into the ER and by the plasma membrane calcium ATPase (PMCA) pump to the extracellular space [12]. Such rapid clearance keeps the cytosolic calcium at low concentration to allow further signal production.

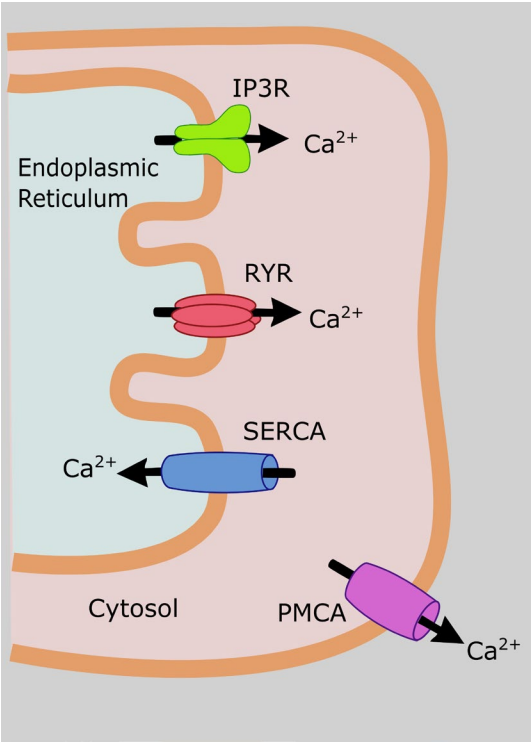


**Figure 1. Calcium movement through channels and pumps in the endoplasmic reticulum and the cytosol.** Shown are the IP3 receptor, RY receptor, SERCA pump and PMCA pump. Arrows represent direction of calcium movement.

The ER represents the initial compartment for newly synthesized proteins to get folded and modified post-translationally. Newly formed polypeptide chains enter the ER through channels called translocons [13]. Once the polypeptide chain starts to emerge into the ER lumen, chaperones rapidly attach to specific domains to keep the chain in a folding-competent state and to prevent it from spontaneous misfolding and aggregation [14]. There are two main chaperone systems in the ER; the calnexin/calreticulin system and the Hsp70 (BiP) system [14]. The calnexin/calreticulin system mainly assist the folding of glycoproteins, with the help of the protein disulfide isomerase ERp57 [15]. The BiP system plays a major role in the folding of non-glycosylated proteins via cycling between ATP-bound and ADP-bound states [16]. Upon correct folding and oligomerization, glycosylated and non-glycosylated client substrates leave the folding machinery and pass folding inspection check-points, and eventually arrive at the ER exit sites to leave the ER to the Golgi apparatus.

Under normal conditions, the rate of protein folding inside the ER is in harmony with the rate of ER export, so that correctly-folded proteins can easily leave the ER

once they arrive at ER exit sites. Any condition that disrupts this harmony can result in the accumulation of misfolded and unfolded proteins inside the ER leading to ER stress. Such disruption can result from a chronic increase in protein synthesis [17] (such as the case in chronically-stimulated professional secretory cells [18]), depletion of calcium from the ER [8] (which disrupt the functionality of the folding machinery), disruption of the oxidizing environment of the ER that is required for disulfide-bond formation [19] or inhibition of ER export [20]. The resulting imbalance between the accumulated unfolded and misfolded proteins and the available ER chaperones induces the activation of the unfolded protein response (UPR). Such an adaptive response aims to relieve ER protein overloading via inhibiting new protein synthesis and improving protein folding, export and degradation [21]. There are three ER stress sensors that are integral membrane proteins of the ER; namely Ire1α (inositol requiring enzyme 1α), ATF6 (inositol requiring enzyme 1) and PERK (protein kinase RNA (PKR)-like ER kinase). Under non-stress conditions, these sensors are kept inactivated through binding to BiP proteins on the luminal side of the ER [22]. Upon the induction of ER stress, these BiP proteins bind instead to the unfolded proteins, leading to the activation of the stress sensors. These sensors start a transcriptional program involving up-regulation of ER chaperons, folding enzymes, ER-associated degradation (ERAD) machinery, ER export machinery and others [21,22]. If the UPR fails to restore ER homeostasis within a specific time frame, it starts an apoptotic program to get rid of hopeless cells. In conclusion, the maintenance of a functional and unhindered ER export process is essential to keep a healthy secretory pathway with no ER stress, and its improvement would be required to alleviate such stress when it occurs.

When correctly-folded and oligomerized proteins arrive at ER exit sites, they get packed into COPII coated vesicles that bud from the ER to deliver the cargo to the Golgi apparatus. The formation of this coat (figure 2) [23] involves an initial activation of the small GTPase Sar1at ER exit sites by the transmembrane ER protein Sec12 (which has guanine nucleotide exchange activity), leading to insertion of Sar1 into the ER membrane. This is followed by the recruitment of the inner coat subunits Sec23/Sec24 and cargo to form a prebudding complex with Sar1, in which Sec24 contains the attachment sites for transmembrane client cargo proteins and for the receptors for soluble luminal cargo proteins. The outer coat subunits Sec13/Sec31 are then recruited to induce membrane bending and vesicle budding. After the COPII

coated vesicle buds from the ER membrane, it loses most of the coat so that it can fuse with the target membrane [24].

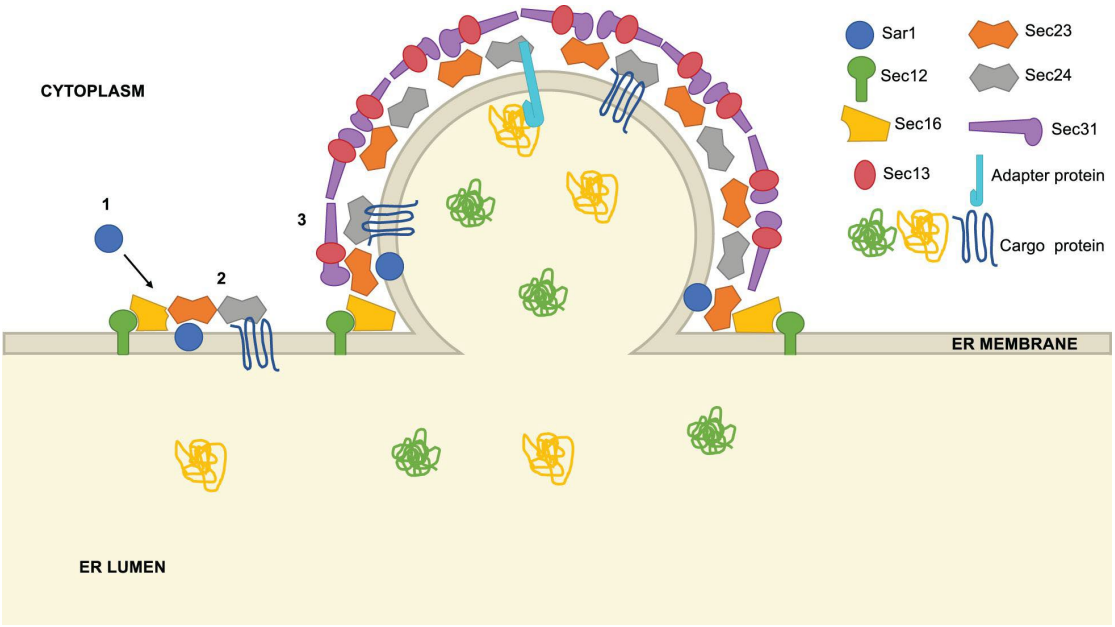


**Figure 2. Overview of COPII vesicle formation.** COPII vesicle formation proceeds through a series of steps: (1) Sar1 is recruited to the ER membrane at ER exit sites (ERES), marked by Sec16. Using the GEF Sec12, Sar1 exchanges GDP for GTP and inserts an α-helix into the ER membrane, promoting curvature. (2) Sec23 and Sec24 heterodimers are recruited to ERES, binding Sar1 and cargo to form the pre-budding complex. Cargo is loaded into the forming vesicle through direct interaction with Sec24, interaction with a Sec24-binding adaptor protein or bulk flow. (3) Lastly, Sec13 and Sec31A heterotetramers assemble around the forming vesicle, promoting further membrane curvature and scission. (**figure adapted from:** Bisnett BJ, Condon BM, Lamb CH, Georgiou GR, Boyce M. Export Control: Post-transcriptional Regulation of the COPII Trafficking Pathway. Front Cell Dev Biol. 2021 Jan 12;8:618652. doi: 10.3389/fcell.2020.618652.)

Importantly, the ER export process is regulated by several cytosolic proteins [23], including the calcium-sensitive regulatory proteins apoptosis-linked gene 2 (ALG-2) and peflin (PEF protein with a long N-terminal hydrophobic domain). ALG-2 is a 22 kDa calcium-binding protein that belongs to the penta-EF-hand protein family with five repetitive EF-hand motifs [25,26]. It was shown that ALG-2 can change its conformation upon exposure to calcium [25,26]. It was also shown that, in the

presence of calcium, ALG-2 can bind to and stabilize the outer coat subunit Sec31A (the homologue that is widely expressed in various cell types, in contrast to Sec31B) at ER exit sites [27,28], and this in turn stabilizes the interaction of Sec31A with the inner coat subunit Sec23 [29]. Peflin is a 30-kDa protein that represents another member of the penta-EF-hand protein family with five repetitive EF-hand motifs, and it was found to be the most similar to ALG-2 in this family [30]. It is known that members of this family exist as homodimers and heterodimers. Using immunoprecipitation and western blotting studies, peflin was shown to interact with ALG-2 to form heterodimers in the absence of calcium, and this interaction was disrupted when calcium was added [31]. On the other hand, peflin was unable to form homodimers either in the presence or absence of calcium, in contrast to ALG-2 that was able to homodimerize in a calcium-stimulated manner [31]. Later, through using truncated mutants, it was shown that the interaction between ALG-2/peflin in heterodimers and between ALG-2/ALG-2 in homodimers involves the fifth-EF-hand (EF-5) regions of both proteins [32]. It was also shown that these EF-5 dependent interactions stabilize both proteins and inhibit their rapid proteasomal degradation [32].

Calcium has been shown to regulate protein transport at different parts of the secretory pathway, including exocytosis [33], intra-Golgi transport [34,35], and Golgi-to-ER retrograde transport [34]. This, in addition to the calcium-stimulated interactions of ALG-2 with the COPII coat at ER exit sites [27,28] and the calcium-induced breakage of ALG-2/peflin heterodimers [31], prompted investigators to examine whether calcium can regulate ER-to-Golgi transport and the possible involvement of ALG-2 and/or peflin in such regulation. One of the earliest studies using semi-intact cells concluded that the maintenance of physiological levels of free $Ca^{2+}$ in the cytosol is essential for efficient ER-to-Golgi transport, since cytosolic calcium depletion could severely inhibit this transport step, and the re-introduction of calcium to the physiological levels resulted in transport recovery [36]. Another study reported that ER calcium depletion could inhibit ER-to-Golgi transport of correctly-folded cargo proteins, and elucidated the involvement of ALG-2-Sec31A interactions on the cytosolic side of ER membrane, suggesting that calcium released from the ER may regulate this step through this interaction [37]. Later, investigators found that peflin (which can stably exist only as a heterodimer with ALG-2 [31]) had an inhibitory effect on ER-to-Golgi protein transport and its depletion could improve

ALG-2 and Sec31A targeting to ER exit sites and their interactions, and could improve transport, further supporting a regulatory role for peflin and ALG-2-Sec31A interactions in transport [38]. This led to a suggested model of regulation (figure 3) in which calcium may cause the breakage of ALG-2/peflin heterodimers and the formation of ALG-2/ALG-2 homodimers which may in turn bind to and stabilize Sec31A at ER exit sites leading to improvement of ER export and ER-to-Golgi transport [38].

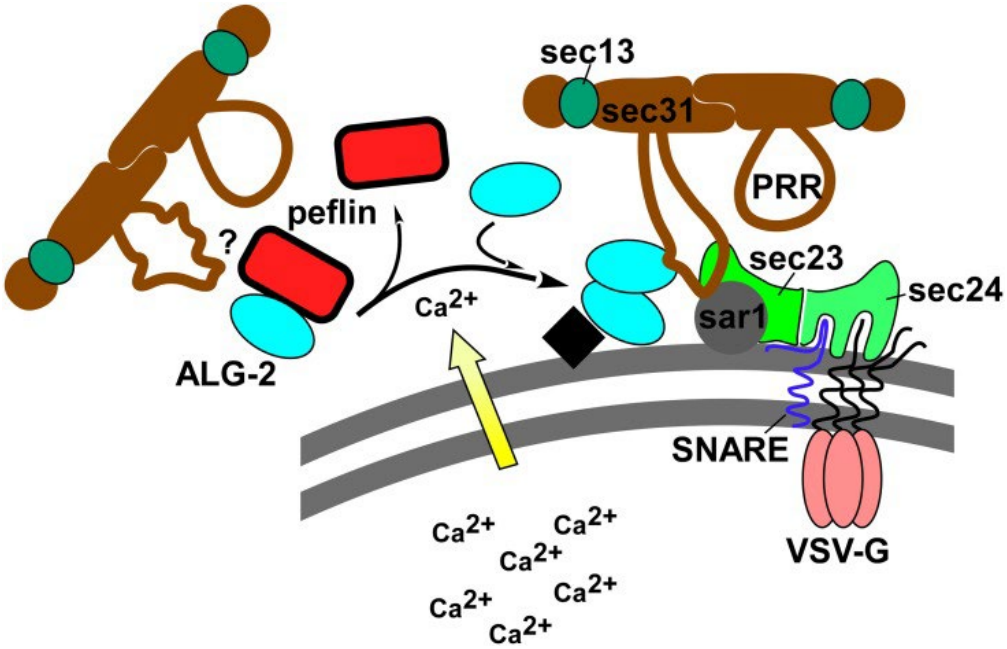


**Figure 3. Model for peflin regulation of ER-to-Golgi transport.** Peflin exists as a heterodimer with its binding partner ALG-2. In the presence of calcium peflin dissociates, allowing ALG-2 to homodimerize and undergo $Ca^{2+}$-dependent binding to the proline rich region (PRR) of Sec31A. ALG-2 binding to the PRR activates the PRR for interactions with inner shell components sar1 and sec23, which stabilizes the coat assembly on the membrane. These events may increase ER-to-Golgi transport. It is not known whether the peflin-ALG-2 heterodimer binds the PRR region and affects its activity ("?" to left of heterodimer). The black square represents a hypothetical docking site for ALG-2 at the ERES. (**figure adapted from** Rayl M, Truitt M, Held A, Sargeant J, Thorsen K, Hay JC. Penta-EF-Hand Protein Peflin Is a Negative Regulator of ER-To-Golgi Transport. PLoS One. 2016 Jun 8;11(6):e0157227. doi: 10.1371/journal.pone.0157227)

All these results reflect the regulation of ER-to-Golgi transport by steady-state levels of calcium in cells. However, studies also tried to investigate whether calcium signaling beyond the steady-state level could regulate this transport step. In the semi-intact cell system used by Beckers and Balch [36], they reported that raising the concentration of free $Ca^{2+}$ in the cytosol beyond the physiological level could decrease the efficiency of transport. A recent study demonstrated that treating different cell types with different calcium mobilizing agents (histamine, ATP, BHQ) for a long time (1-2.5 hours) could produce different PEF protein-dependent changes in transport, and these changes were dependent on the pattern of changes in cytosolic calcium [39]. Treatments that induced sustained cytosolic $Ca^{2+}$ oscillations through the treatment course (figure 4A) led to $Ca^{2+}$-activated depression of ER export (CADEE), which was associated with decreased targeting of Sec13/Sec31A and increased targeting of peflin to ER exit sites and which was prevented by knockdown of ALG-2. On the other hand, treatments that induced an immediate single calcium surge with rare or no further oscillation (figure 4B) led to a $Ca^{2+}$-activated enhancement of ER export (CAEEE), which was also prevented by knockdown of ALG-2. This suggested that different patterns of calcium signals in the cytosol can either increase or decrease ER-to-Golgi transport in a mechanism involving the PEF proteins. However, it remains unknown how the calcium-dependent dynamics of ALG-2 and peflin at ER exit sites results in changes to the outer coat and its functions in cargo export.

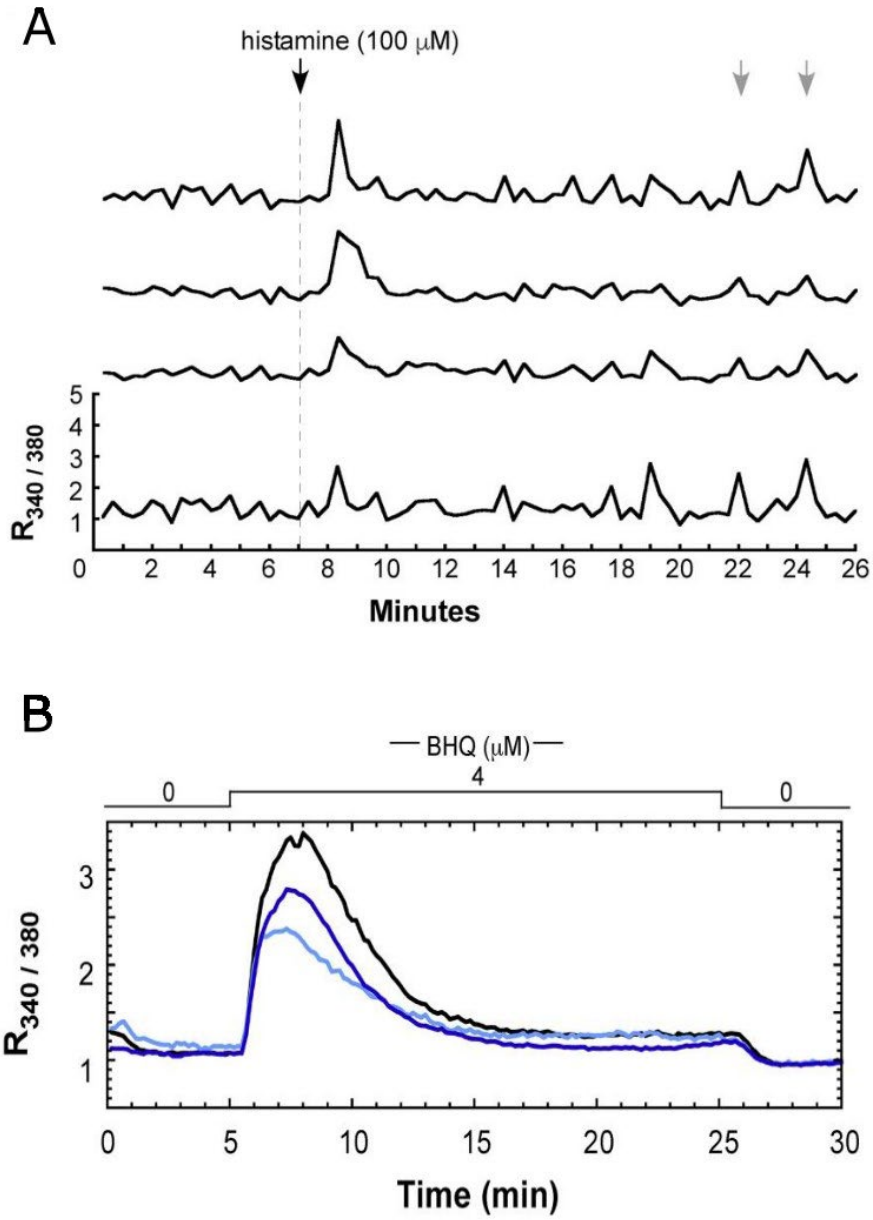


**Figure 4. cytosolic calcium patterns associated with CADEE and CAEEE. A.** Calcium patterns associated with CADEE: representative single-cell cytosolic $Ca^{2+}$ traces measured using FURA-2 in wild-type NRK cells. Traces are from the same coverslip. 100 μM histamine was added after 7 min of perfusion in growth medium. Nonresponding cells were present but are not shown. Gray arrows mark synchronous $Ca^{2+}$ oscillations in multiple cells. **B.** Calcium patterns associated with CAEEE: example FURA-2 traces of NRK cells exposed to 4 μM BHQ, cells were recorded during perfusion with media successively lacking, containing, and then lacking BHQ. (**adapted from** Sargeant J, Seiler DK, Costain T, Madreiter-Sokolowski CT, Gordon

DE, Peden AA, Malli R, Graier WF, Hay JC. ALG-2 and peflin regulate COPII targeting and secretion in response to calcium signaling. J Biol Chem. 2021 Dec;297(6):101393. doi: 10.1016/j.jbc.2021.101393.)

Since calcium is known to regulate several steps in the late secretory pathway, and since the calcium sensitive regulatory proteins ALG-2 and peflin are known to function at ER exit sites, we hypothesized that calcium may regulate ER export as well through these proteins. In the current study, we attempted to investigate the effect of inducing a single transient cytosolic calcium pulse on ER-to-Golgi transport and the associated changes in the dynamics of ALG-2, peflin and COPII coat proteins at ER exit sites. More specifically, we wanted to know whether a single calcium pulse could induce long-lasting functional changes at ER exit sites, such as their ability to concentrate cargo. We also wanted to test how a calcium pulse would affect targeting of both ALG-2 and peflin to ER exit sites over time and whether and when these events would lead to changes in COPII outer coat recruitment.

## Chapter 2: Results

**Calcium enhances cargo recruitment to ERES.** We sought to examine the effect of a transient cytosolic calcium pulse on protein transport in the early secretory pathway. For this purpose, we used the reversible Sarco-Endoplasmic Reticulum Calcium ATPase (SERCA) pump inhibitor 2,5-Di-(t-butyl)-1,4-hydroquinone (BHQ). BHQ will induce the mobilization of calcium from the ER to the cytosol until it is washed out. We first transfected normal rat kidney (NRK) cells derived from kidney epithelia with the cargo protein GFP-$FM_4$-VSV-$G_{tm}$. This cargo contains a conditional aggregation domain, FM4, that aggregates in the ER and prevents export until a small-molecule drug, AP21998 (also called D/D Solubilizer), is provided, causing synchronous ER export and transport to the Golgi [40]. Cargo-transfected cells were exposed to BHQ for 3 minutes, washed with PBS and incubated in full DMEM medium for 60 minutes at 37 ºC before inducing transport. This incubation was included to allow any $Ca^{2+}$-dependent events to modify ERES structure/function. For the cargo recruitment to ER exit sites incubation, the cells were then exposed to D/D solubilizer for 60 minutes at 10 ºC. Incubation at this low temperature allows the cargo proteins to be sorted into ER exit sites but blocks vesicle scission and transport to the Golgi, and represents a characterized technique to measure cargo recruitment at ER exit sites [41]. Cells were then fixed and imaged by confocal microscopy. Through visual inspection of the images of the cells (figure 5A), we noticed increased intensity of intracellular spots, representing VSV-G accumulated at ER exit sites, in BHQ treated cells compared to vehicle DMSO-treated cells. This suggested an increased cargo recruitment to ER exit sites one hour after a transient calcium pulse. We then used imageJ software to analyze the images and to quantify changes in cargo intensity at ER exit sites. We found a significant 30% increase in the accumulation of cargo proteins at these sites after BHQ treatment compared to DMSO-treated control cells (Figure 5B). This indicates that a short, well-defined calcium pulse can indeed significantly enhance the sorting of client cargo proteins at ER exit sites.

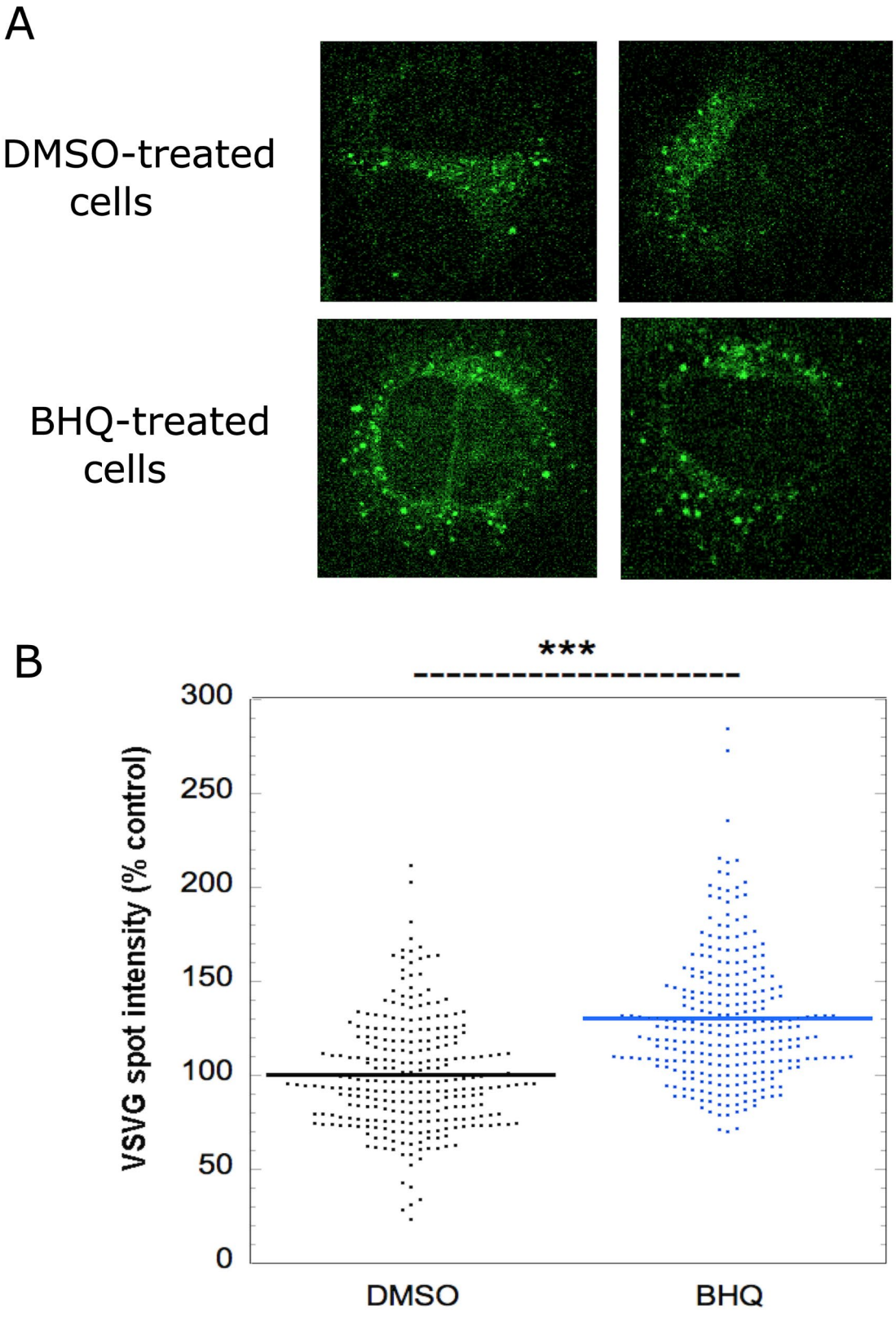


**Figure 5. Effect of a transient calcium pulse on cargo recruitment to ER exit sites in NRK cells.** NRK cells transfected with GFP-$FM_4$-VSV-$G_{tm}$ cargo proteins were treated with BHQ for 3 minutes. 1h later, cargo proteins were allowed to undergo cargo accumulation at ERES during exposure to D/D solubilizer for 60 minutes at 10

ºC. Confocal microscopic images were analyzed using imageJ. **A.** Representative confocal images of vehicle DMSO-treated and BHQ-treated cells, showing the fluorescent cargo at ER exit sites. Each panel contains one NRK cell. **B.** Graph of cargo recruitment to ER exit sites in DMSO-treated and BHQ-treated cells. Spot maximum intensity (representing cargo accumulated at ER exit sites minus background) was measured in BHQ-treated and control DMSO-treated cells (4-7 bright spots analyzed per cell, ~ 55 cells per condition). *** represents p<.0005 in a two-tailed Student's T-test assuming unequal variance.

We repeated this experiment using a different cell type from a different species. We used U2OS cells, which represent an osteosarcoma cell line derived from humans [42]. Similar to NRK cells, we found a significant increase in cargo protein accumulation at ER exit sites 1 hour after BHQ treatment, compared to DMSO-treated control cells (Figure 6). This indicates that the phenomenon is common to different cell types. Notably, we found a greater magnitude of increase in cargo accumulation at ER exit sites after BHQ treatment in U2OS cells compared to NRK cells (compare figures 5 and 6, 30% increase in NRK cells versus 60% increase in U2OS cells). To summarize Figures 5 and 6, we have established that a short, well-defined $Ca^{2+}$ pulse can alter ERES structure/function to produce more aggressive sorting of client cargo into export sites. Furthermore, the altered functionality of ERES can persist for at least one hour following the elevated calcium.

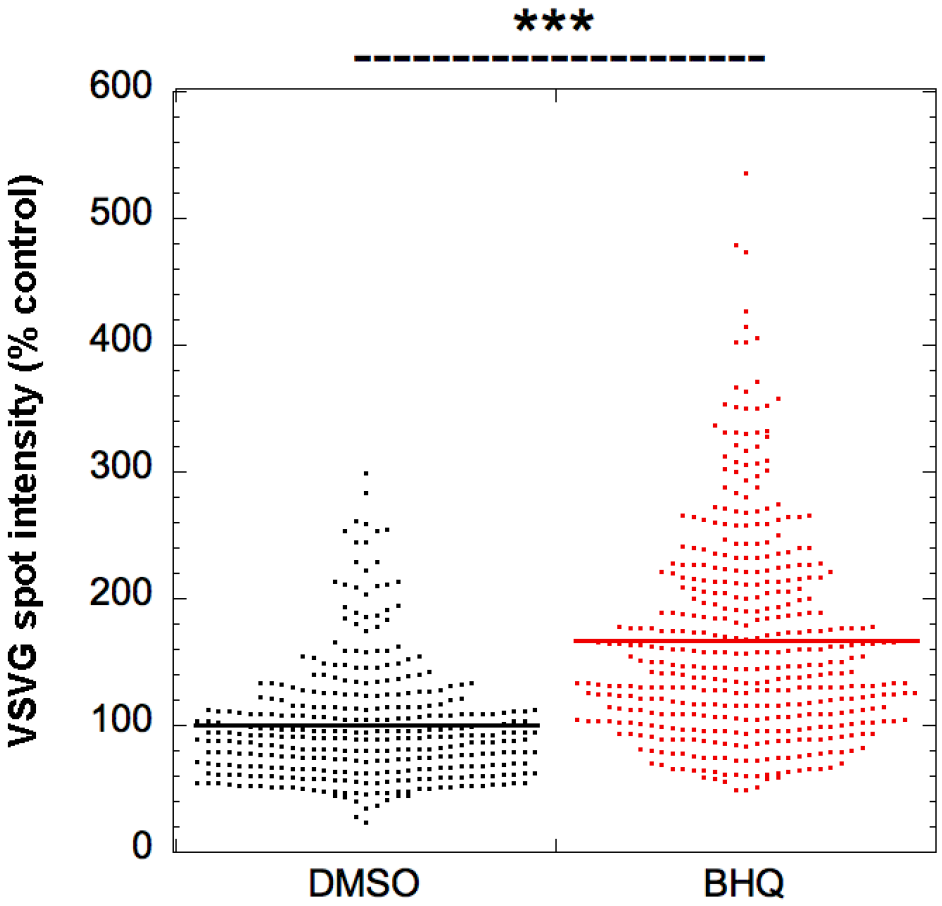


**Figure 6. Effect of a transient calcium pulse on cargo recruitment to ER exit sites in U2OS cells.** U2OS cells transfected with GFP-FM4-VSV-Gtm cargo were treated and analyzed as in NRK cells in Figure 5. Shown is a graph of maximum spot intensity at ER exit sites in vehicle DMSO-treated and BHQ-treated cells, representing cargo recruitment to ER exit sites. *** represents p<.0005 in a two-tailed Student's T-test assuming unequal variance.

**A transient calcium pulse induces long-lasting recruitment of COPII outer coat subunits Sec13 and Sec31A.** $Ca^{2+}$-dependent ERES changes have been suggested to arise via the $Ca^{2+}$ adaptor ALG-2 stabilization of the COPII outer coat [27, 28]. However, we are lacking information about the kinetics of outer coat recruitment relative to ALG2 recruitment and calcium. Therefore, we sought to perform live microscopy experiments at a single-cell level to detect changes in the recruitment of ALG-2 and the outer coat proteins Sec13 and Sec31A to ER exit sites during and after a transient calcium pulse. NRK cells transfected with mRuby2-ALG-2, Sec13-GFP and Halo-Sec31A were exposed to BHQ in complete DMEM for 3

minutes followed by exposure to complete DMEM without BHQ for up to 30 minutes using a heated perfusion system. Confocal images were collected every minute for all three proteins at target cells to produce time-lapse images. Visual inspection revealed a prominent, transient increase in the intensity of ALG-2 (representing protein recruitment to exit sites) during the calcium pulse (Figure 7A). However, the effects on Sec13 or Sec31A were not as prominent. We used imageJ software to analyze changes in the intensity of the three proteins over time. We found distinct patterns of changes for the three proteins over the treatment time-course. For ALG-2 (figure 7B), there was an immediate large increase in its intensity during BHQ treatment before returning to a new plateau near baseline yet statistically higher than the baseline for the entire 30 minutes after BHQ wash out. For Sec13 and Sec31A (figure 7C and 7D), there was a more subtle but still clearly visible increase in the intensities of both proteins during the BHQ treatment, unitemporally with ALG-2. Later, their intensities exhibited a higher than baseline plateau that represented significant, sustained recruitment relative to the starting levels. This data demonstrates a mechanism by which a transient calcium pulse can produce longer-lasting remodeling of ER exit site proteins to facilitate greater cargo recruitment to export sites. Since Sec13 and Sec31A were retained relatively more than ALG-2 during the sustained phase, it seems possible that another targeting mechanism other than the sustained physical presence of ALG-2 might be involved in their long-term retention at ERES.

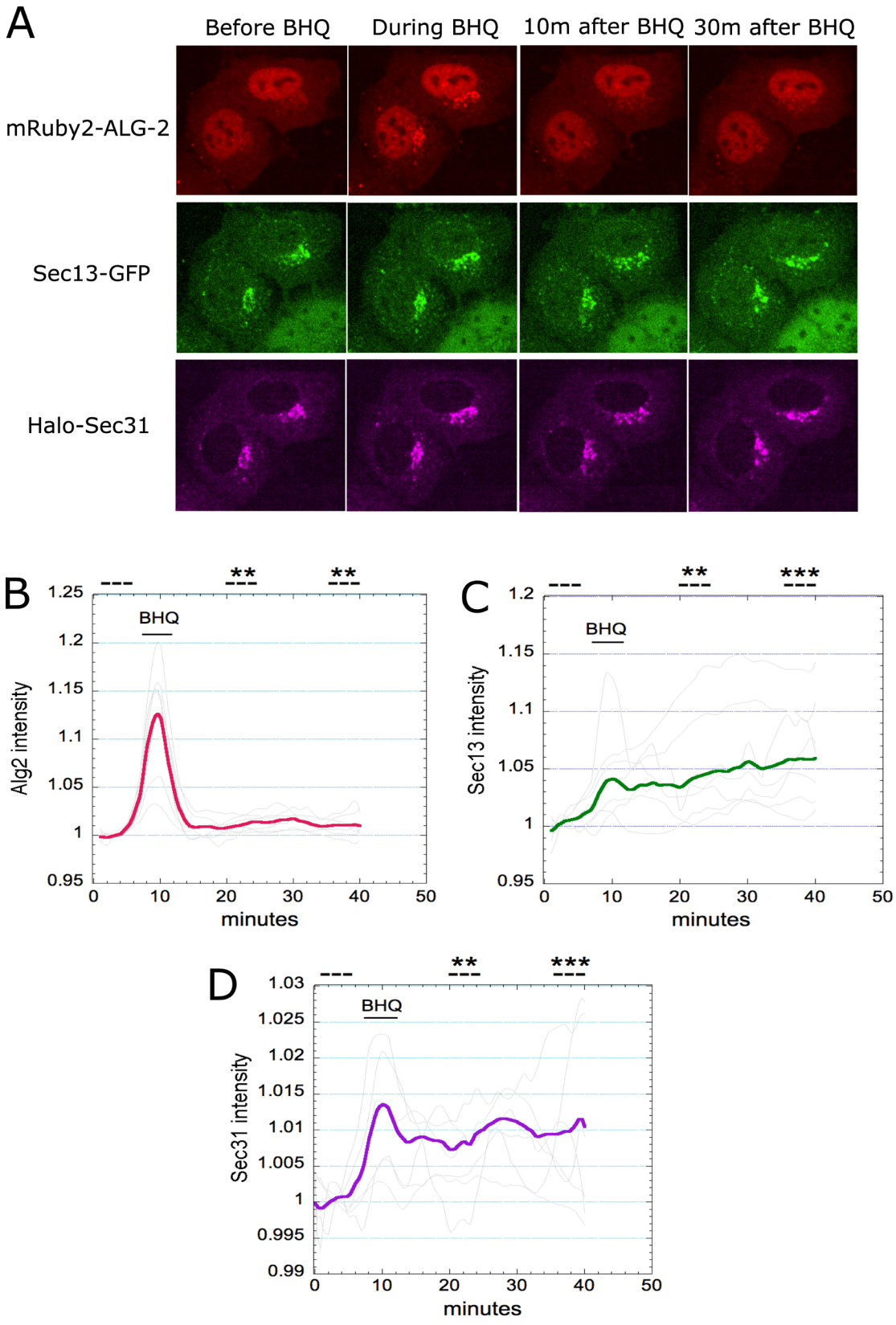


**Figure 7. Live microscopy of cells during and after a transient calcium pulse.** NRK cells were transfected with mRuby2-ALG-2, Sec13-GFP and Halo-Sec31A, placed in a heated perfusion system on a confocal microscope, and treated with BHQ for 3 minutes followed by full DMEM medium for 30 minutes. **A.** Confocal

microscopic images from the time-lapse showing changes in the intensities of ALG-2, Sec13 and Sec31A at different time points during and after the transient calcium pulse. B-D. Graphs generated after analyzing the live movie frames using imageJ software to detect changes in the intensities of ALG-2 **(B)**, Sec13 **(C)** and Sec31A **(D)**. Graphs represent the mean intensity of a uniform region of interest encircling the main cluster of ERES in the perinuclear area in consecutive images. Intensities from each trace were divided by their initial intensity to normalize the start of each trace to a value of 1. Images were recorded at a rate of 1 frame per minute. Individual cell intensities are shown as faint lines, while the mean values are shown as bold lines. Dotted lines above the plot indicate comparisons of groups of consecutive intensity values at different times versus before adding BHQ. *** represents $p<.0005$, ** represents $p<.005$ in a two-tailed Student's T-test assuming unequal variance.

**Both ALG-2 and peflin transiently target to ERES during and following a transient calcium pulse**. We next sought to monitor the dynamics of endogenous ALG-2 and its binding partner/regulator peflin at ERES. ALG-2 can target to ERES as either an ALG-2 homodimer or an ALG-2/peflin heterodimer [39]. Peflin only binds ERES with ALG-2. While ALG-2 is known to bind ERES immediately in response to $Ca^{2+}$ [29], nothing is known about how the ALG-2/peflin heterodimer responds to $Ca^{2+}$ in the cell. We hypothesized that $Ca^{2+}$ should induce the dissociation of these heterodimers at exit sites, similar to previous in vitro results [31]. Furthermore, tagged peflin constructs do not bind ERES authentically, so immunofluorescence of endogenous peflin was necessary to answer the question. This also provided the opportunity to confirm the changes in ALG-2 recruitment to ERES seen in live microscopy (Figure 7) using endogenous ALG-2 . NRK cells were treated with BHQ for 3 minutes, washed with PBS and then incubated in OptiMEM for up to 60 minutes. Cells were then fixed and immuno-stained with ALG-2 antibodies and peflin antibodies. Confocal microscopic images were collected at various time points during and after BHQ treatment. Visual inspection of the anti-peflin images was optimal because of the high specificity of the peflin antibody (Figure 8A). Peflin spots were shown to co-localize extensively with ERES [39]. We noticed that the intensity of the peflin spots at ER exit sites increased after 1 minute of BHQ treatment, but were dramatically reduced after 3 minutes of BHQ treatment before re-appearing again at later time points. We then analyzed changes in the intensities of both ALG-2

and peflin during and after the calcium pulse using imageJ software. Analysis of the peflin dynamics is shown in Figure 8B. This confirmed a dramatic increase at 1 minute followed by below-baseline recruitment at 3 minutes of BHQ treatment, followed by a gradual recovery over 60 minutes of peflin at ERES to greater than initial levels. Since peflin requires ALG-2 for binding ERES, we assume that these binding dynamics represent the ALG-2/peflin heterodimer species. These results imply that the ALG-2/peflin heterodimer is initially stimulated to bind ERES by a $Ca^{2+}$ pulse, which contradicts previous in vitro studies which suggested that the ALG-2/peflin heterodimer dissociates in the presence of $Ca^{2+}$. If the heterodimer dissociates in response to $Ca^{2+}$ in the cell, it must do so only after an initial surge of ERES binding.

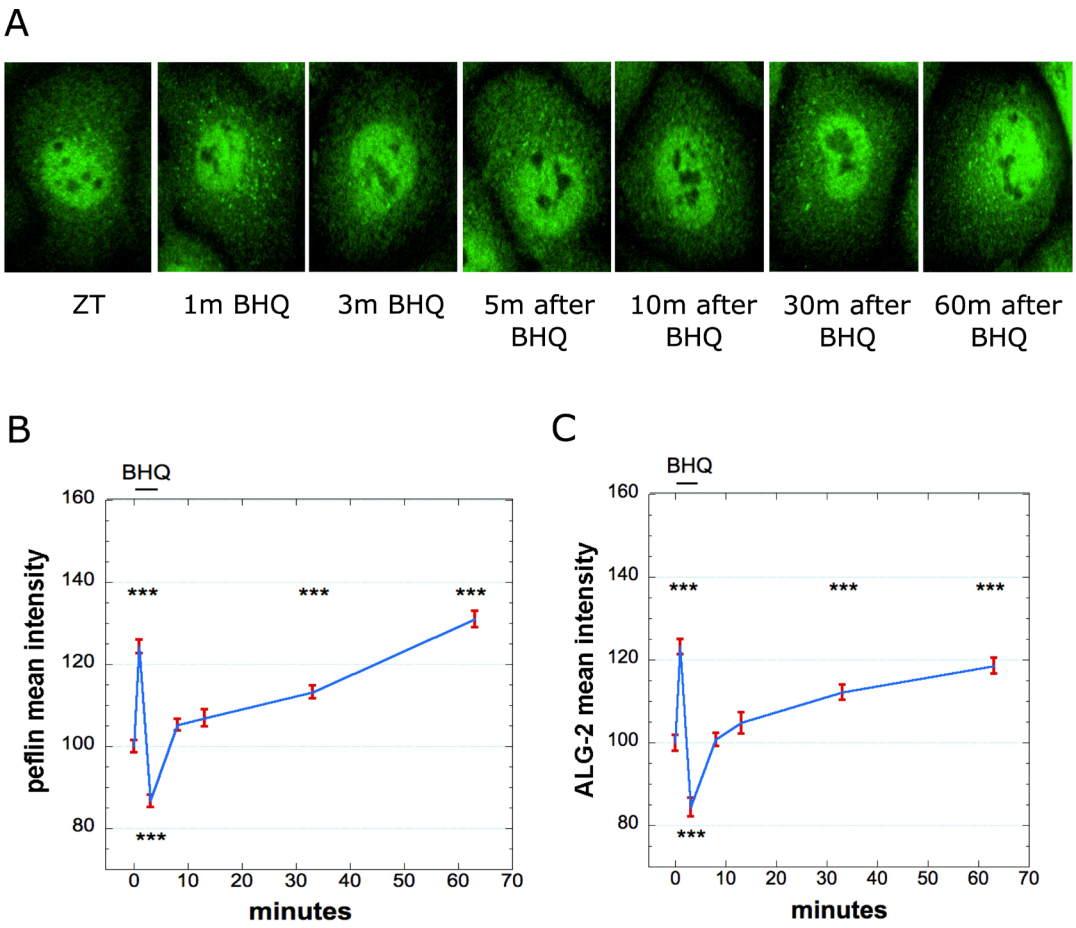


**Figure 8. Immuno-fluorescence of ALG-2 and peflin during and after a transient calcium pulse.** NRK cells grown overnight in OptiMEM were treated with BHQ for 3 minutes, followed by incubation in OptiMEM for up to 60 minutes. **A.** Confocal microscopic images of peflin at different time points after immuno-staining. **B.** Graph

of analyzed peflin changes and **C.** ALG-2 changes during and after the calcium pulse, using imageJ software. Maximum intensity of individual peflin spots and colocalizing ALG-2 spots minus background were analyzed. 4-7 bright spots were analyzed per cell, ~ 45 cells per condition. *** represents $p<.0005$ in a two-tailed Student's T-test assuming unequal variance.

ALG-2 antibody decorated authentic ALG-2 at ERES as well as some nonspecific sites. To overcome the problem of the non-specific staining during the quantitation, we only analyzed the intensity of ALG-2 spots that co-localized with peflin spots. Results (Figure 8C) showed that ALG-2 changes in the fixed immuno-fluorescence studies were basically similar to the changes seen in live microscopy studies (figure 7B) with the exception of some alterations at specific time points. Initially, ALG-2 intensity increased significantly at 1 minute during BHQ treatment, similar to the initial peak seen in live microscopy results. This was followed by a significant decrease below baseline, a result not seen in live microscopy results. ALG-2 intensity then increased again above baseline to a significant level 30-60 minutes after the BHQ treatment. Thus, the main difference between the live (Figure 7) and endogenous (Figure 8) studies of ALG-2 is the strong drop in intensity seen after the initial calcium-induced ALG-2 peak in the endogenous protein study.

Comparison of the dynamics of both peflin and ALG-2 showed that changes in both proteins were very similar at different time points (Figure 8B and 8C). This may suggest that the primary species monitored was a heterodimer of ALG-2 and peflin. That the heterodimer binds ERES at least transiently in response to $Ca^{2+}$, as opposed to dissociating [31] has important consequences because it allows the possibility of a $Ca^{2+}$-stimulated wave of mono-ubiquitylation at ERES; the ubiquitylation-promoting activity of ALG-2 and peflin has recently been shown to require the heterodimer of ALG-2 and peflin [43]. This enzymatic activity could be involved in the long-term remodeling of ER exit sites for greater cargo recruitment (Figures 5 and 6).

## Chapter 3: Discussion

In this study, we examined the effect of inducing a transient calcium pulse on protein transport dynamics in the early secretory pathway. Such a pulse could naturally be generated in cells by various stimuli including regulated exocytosis. During exocytosis, calcium enters the cell through calcium channels to stimulate the fusion of the secretory vesicles with the plasma membrane [44]. However, new protein synthesis would be necessary to maintain adequate stores of the secreted proteins to support repeated secretion. For example, when pancreatic beta cells are stimulated by high glucose, mitochondria start to increase ATP production which leads to an increase in the ATP:ADP ratio, blocking K+ATP-sensitive channels, resulting in membrane depolarization and the influx of calcium through voltage-gated calcium channels, resulting in the exocytosis of insulin-loaded vesicles [45]. However, glucose also stimulates insulin gene transcription, and mRNA stability and translation [45,46]. This prompted us to investigate whether such a calcium pulse could also improve the secretory pathway, especially ER-to-Golgi transport (which is an important rate-limiting step in the secretory pathway), to provide increased cargo capacity. First, we exposed cells to the SERCA pump inhibitor BHQ for 3 minutes to induce a short calcium pulse, and then traced changes in the intensity of cargo proteins in the ER and the Golgi. We found evidence of increased Golgi to ER ratio of intensities (representing an increase in cargo concentration in the Golgi with a concomitant decrease in the ER) 1 hour following BHQ exposure in both NRK and U2OS cells (results not shown), indicating an increase in the rate of ER-to-Golgi transport. However, these promising results were difficult to reproduce. One possible cause for such difficulty could be the inability to preserve the Golgi architecture following the disruption of calcium homeostasis inside cells. Through visual inspection of microscopic images, we noticed that the Golgi apparatus appeared fragmented following BHQ treatment. This is reminiscent of the Golgi fragmentation seen in cells lacking the secretory pathway $Ca^{2+}$-ATPase pump type 1 (SPCA1), which pumps calcium into the Golgi apparatus [34], suggesting that calcium homeostasis is essential to keep a healthy functional Golgi apparatus.

To overcome this problem, we switched to a different protocol to eliminate the need for including the Golgi apparatus in the transport analysis. We induced cargo transport while incubating cells at 10 ºC. This low-temperature incubation allows

cargo sorting and translocation to ER exit sites, but doesn't allow actual transport to the Golgi. By analyzing the intensities of the brightest fluorescent spots (representing cargo accumulated at ER exit sites), we found a significant increase in cargo sorting at ER exit sites 1 hour following the calcium pulse in different cell types (figures 5, 6), suggesting that the calcium pulse may induce long-lasting changes at ER exit sites allowing for increased function for transport. We found a greater magnitude of increase in U2OS cells than in NRK cells, perhaps because U2OS osteosarcoma cells may have a more developed and equipped secretory pathway and hence more effector proteins, compared to NRK cells which are kidney epithelial cells that are not involved in regulated secretion, and thus have a less-equipped secretory pathway.

In a previous study from our laboratory, it was shown that NRK cells exhibited $Ca^{2+}$-activated enhancement of ER export (CAEEE) after treatment with BHQ for 2.5 h [39]. CAEEE was associated with a BHQ-induced pattern of calcium signaling involving an initial surge of cytosolic calcium followed by returning to an above baseline plateau (figure 4B). The study suggested that this pattern is responsible for CAEEE. In the current study, we only induced the initial surge of cytosolic calcium and excluded the remaining above baseline plateau, and we observed CAEEE after 1h, indicating that such phenomenon requires only the initial transient surge of calcium in the cytosol. Our results hence show for the first time that functional changes at ERES can persist for a long time following a single $Ca^{2+}$ event. It was also shown previously that BHQ-induced CAEEE was dependent on the PEF proteins, since knock-down of ALG2 prevented the enhancement of ER export [39]. In the current study, we instead examined changes in the dynamics of ALG2, peflin and outer coat proteins at ER exit sites during and after BHQ treatment, using live and fixed cell fluorescence microscopy studies. Results showed a two-phase response in both studies, with the first phase occurring during BHQ treatment and the second phase occurring after BHQ washout. In the live-cell studies, we could not trace changes in peflin due to the absence of a functional fluorescent peflin construct. So, we traced ALG-2, Sec31A and Sec13. For all three proteins, we found an initial increase in their intensities at ER exit sites during BHQ treatment (figure 7B, C, D), which is concomitant with the calcium surge in the cytosol. The increase in Sec31A (and its binding partner Sec13) unitemporally with ALG-2 is consistent with the previously reported calcium-induced binding of ALG-2 to Sec31A and its stabilization at ER exit sites [27, 28]. However, to our knowledge the kinetics of outer coat recruitment by calcium and ALG-2 had

never been documented. Our study uniquely shows that outer coat recruitment is initiated unitemporally with calcium but persists well after the calcium has been cleared.

Since previous literature has indicated that only ALG-2 homodimers bind Sec31A in response to calcium, and that calcium induces dissociation of ALG-2-peflin heterodimers, we expected peflin intensities at ER exit sites to drop upon BHQ addition. However, when we performed fixed-cell immunofluorescence studies of endogenous proteins, we found that the initial increase in ALG-2 intensity at ER exit sites was accompanied by a similar increase in peflin intensity (figure 8B, C), which opposes the previously suggested notion that calcium induces the dissociation of ALG-2/peflin heterodimers. This notion came from in vitro studies of purified proteins [31], which could lack other intracellular proteins that may affect the heterodimer stability during calcium signaling. The previous in vitro studies also did not address the kinetics of dissociation relative to calcium. Our studies on the other hand indicate concomitant increases in ALG-2 and peflin during the calcium pulse, suggesting that heterodimers are targeted to ER exit sites by calcium. This does not exclude the targeting of ALG-2/ALG-2 homodimers as well. It also suggests that the ALG-2/peflin heterodimers could be the entity responsible for the stabilization of Sec31A at ER exit sites, which opposes the proposed model that ALG-2/ALG-2 homodimers are the responsible entity (figure 3) [38]. Further studies would be required to assign functions to homodimers versus heterodimers during calcium signaling.

One obvious discrepancy in our data between the live-cell and fixed-cell immunofluorescence studies is that, in the fixed cells, there was a strong drop below baseline in ALG-2 intensity following the initial increase, which was not observed in the live cells (figures 8C and 7B). One possible explanation could be that the immunofluorescence studies involve more steps like fixation, permeabilization, primary and secondary immunostaining, perhaps making them more prone to errors or inaccuracy. However, the strong drop in ALG-2 intensity was accompanied by an identical drop in peflin intensity, which could suggest that it may be a true heterodimer event. This could be related to the mode of addition and washing of BHQ which was different between live-cell and fixed-cell studies. In the live-cell studies, there was a more gradual addition and washing of BHQ through the perfusion system, while in the fixed-cell studies, the BHQ delivery and washout steps were more abrupt.

It is possible that the abrupt clearance of calcium from the cytosol resulted in a sudden destabilization of the ALG-2/peflin heterodimers at ER exit sites. Modifying the delivery and washout system in the live-cell studies could help clarify this discrepancy. Another possible explanation for the discrepancy could be that the tagged ALG-2 construct used in the live-cell studies behaves differently from the endogenous protein detected in the immunofluorescence studies. Alternatively, the over-expression above endogenous levels in the live-cell studies could cause the distinct behavior observed in those studies.

The second, or post-calcium phase of the response was similar in both the live-cell and fixed-cell studies, though the post-calcium ALG-2 recruitment was quantitatively greater in the fixed-cell than in the live-cell studies. For ALG-2, the mean intensity at ER exit sites in the live-cell studies returned to a new plateau which was significantly higher than the baseline (figure 7B). In the fixed-cell studies, both ALG-2 and peflin intensities increased above the baseline during the post-calcium phase after their initial increase followed by strong drop in their intensities (figures 8B, 8C). Similar to ALG-2, Sec13 and Sec31A returned to a new plateau significantly higher than the baseline for the entire post-calcium phase (figure 7C, D). This suggests the occurrence of long-lasting changes at ER exit sites allowing for increased recruitment of the COPII coat to these sites. It also suggests that during the calcium surge, ERES structure/function is remodeled in a way that persists beyond the cytosolic calcium pulse. Importantly, the fixed-cell studies showed that the changes in the intensities ALG-2 and peflin were almost identical and occurred roughly to the same extent in the first and second phases. This suggests that ALG-2/peflin heterodimers could be physically involved in the long-lasting changes occurring at ER exit sites.

An intriguing mechanism that may be involved is the mono-ubiquitylation of Sec31A with the aid of ALG-2/peflin heterodimers, which increases upon calcium signaling [43, 47]. In these studies, the ALG-2/peflin heterodimers were shown to form calcium-dependent complexes with the ubiquitin ligase CUL3 and its adaptor KLHL12 ($CUL3^{KLHL12}$) and Sec31A. Both ALG-2 and peflin were shown to be necessary cofactors resulting in the mono-ubiquitylation of Sec31A and peflin. Upon calcium signaling, $CUL3^{KLHL12}$-peflin-ALG-2 was shown to increasingly modify Sec31A, resulting in the addition of a persistent mono-ubiquitylation signal to Sec31A [43]. The mono-ubiquitin signal on Sec31A was suggested to enable the formation of larger COPII vesicles, to increase collagen export from the ER [43, 48]. However, a

more recent study suggests that it may instead shift collagen away from secretion and into a degradation pathway [49]. Based upon these and our results, a possibility is suggested that could allow persistent recruitment of COPII outer coat (Sec31A and Sec13) beyond the calcium surge phase. Perhaps ALG-2/peflin heterodimers target the ER exit sites during calcium signaling where they participate in mono-ubiquitylation of Sec31A and then dissociate and leave these sites, which is supported by the rapid decrease of their intensities immediately after BHQ wash-out. The persistent mono-ubiquitylation signal could lead to persistently increased targeting of outer coat beyond the calcium surge, representing a long-lasting ERES remodeling process. This could help explain the long-lasting changes in cargo recruitment to ERES that we observed in Figures 5 and 6 as well as the long-lasting increases in outer coat recruitment we observed in Figures 7 and 8. Of course, other mechanisms could explain the persistent functional effects of a single calcium pulse, but since ALG-2 and peflin have been implicated in mono-ubiquitylation of ERES components, this represents a hypothesis worth investigation.

In conclusion, a transient cytosolic calcium pulse can induce long-term improvement of cargo sorting at ER exit sites. This pulse can also induce immediate as well as sustained post-calcium recruitment of ALG-2 and peflin, as well as the outer coat subunits Sec13 and Sec31A to ER exit sites, suggesting a regulatory relationship. During the calcium surge, ERES structure/function could be remodeled in a way that persists beyond the calcium per se. The calcium induced recruitment of ALG-2/peflin to ER exit sites may induce structural and/or functional changes resulting in long-term recruitment of the outer coat proteins to these sites.

# Chapter 4: Materials and methods

## Antibodies

Chicken polyclonal anti-ALG-2 and rabbit polyclonal anti-peflin were made and their reaction specificity were characterised in our lab [39]. Anti-ALG-2 were used at a dilution of 1:100, and anti-peflin were used at a dilution of 1:500. For secondary staining, chicken cy3-conjugated secondary antibodies from Jackson ImmunoResearch Laboratories (West Grove, PA) were used at a dilution of 1:300, while rabbit Alexa Fluor$^{TM}$ 488-conjugated secondary antibodies from Invitrogen (Carlsbad, CA; product A11001) was used at a dilution of 1:200.

## Cell culture and transfection

NRK and U2OS cells were thawed and grown for 1-2 days in DMEM containing 4.5 g/L glucose, 10% fetal calf serum (FCS) and 2% penicillin-streptomycin, at 37 ºC and 5% CO2. When cell confluency reached ~ 40-50%, old medium was replaced by 1mL new medium in each well for 30-60 minutes, then a solution containing PolyJet/ DNA mixture was added to the cells for 8-12 hours. Cells were then washed once with PBS and incubated overnight in 2ml complete DMEM. Plasmid constructs used include GFP-FM$_4$-VSVG$_{tm}$ [39], Sec13-GFP [50], Halo-Sec31A [51] and mRuby2-ALG-2 (our lab, unpublished).

## BHQ treatment and cargo concentration at ERES assay

NRK or U2OS cells were transfected with GFP-FM$_4$-VSVG$_{tm}$ as described above. Prior to transport, cells were left in complete DMEM at 37 ºC for 8-12 hours to accumulate the cargo proteins in the ER. Cells were exposed to BHQ or DMSO at a concentration of 4 μM for 3 minutes. Cells were then dipped once in PBS and incubated in DMEM medium for 1 hour at 37 ºC. For the cargo concentration at ERES, cells were transferred to a 10 ºC DMEM medium containing the transport inducer (D/D Solubilizer) for 1 hour to allow cargo to move from the aggregates into ER exit sites. Cells were fixed for 30 minutes by immediately transferring them to 6-well plates containing the fixative (4% paraformaldehyde, 0.1 M sodium phosphate).

For morphological quantitation of cargo recruitment to ERES, confocal microscopic images of cells were collected at random positions of the coverslip. Image files for BHQ and DMSO-treated cells were randomized then analyzed by ImageJ software. We used an ImageJ script developed in our lab (Jacob Lapka) termed Spotify to measure intensity changes at individual ER exit sites. This script uses a region of interest (ROI) composed of two circles; a small circle inside a bigger circle. The small circle encompasses the bright fluorescent spot (representing ER exit sites), while the donut-shaped surrounding circle measures the cytosolic area around the bright spots. The max intensity and the mean intensity were extracted from the small circle and the surrounding circle, respectively. 4-7 of the brightest spots were analyzed in each cell. Around 55 cells were analyzed for each condition. We plotted the max intensity of the small circle after substracting the mean intensity of the surrounding circle.

**BHQ treatment and Immunofluorescence microscopy**

NRK cells were incubated overnight in OptiMEM and treated with BHQ as described above. Then, cells were dipped once in PBS and transferred immediately to the fixative or back to the OptiMEM for various amounts of time before fixation. Cells were always kept at 37 ºC.

For immuno-staining, fixed cells were treated for 40 seconds with 0.2% Triton X-100 in permeabilization solution (1% BSA and 2% normal goat serum in PBS) at room temperature. Cells were then incubated with primary antibodies for 1 hour. Next, cells were washed 3 times with the permeabilization solution for 2 minutes each time. Cells were incubated in the dark with secondary antibodies for 30 minutes at room temperature and then washed again 3 times with the permeabilization solution. Coverslips were mounted in Slow-Fade Gold anti-fade reagent (Invitrogen), sealed on glass slides, and imaged using confocal microscopy.

For morphological quantitation of ALG-2 and peflin dynamics at ERES, images were collected and analyzed using the Spotify script described above. The ROI was placed to encompass the peflin bright spots, and the max intensity of the spot and the mean intensity around the spot were calculated as described above. The same ROI was used to analyze colocalizing ALG-2 spots and to calculate the max intensity of the spot and mean intensity surrounding the spot. 4-7 of the brightest spots were

analyzed in each cell. Around 45 cells were analyzed for each condition. We plotted the max intensity of the small circle after substracting the mean intensity of the surrounding circle for both proteins.

**Live microscopy**

NRK cells transfected with Sec13-GFP, Halo-Sec31A and mRuby2-ALG-2 were incubated with JaneliaFluor 646 for 15-30 minutes to label the Halo tag on Sec31A. Coverslips were then mounted in the perfusion chamber of a spinning disk confocal microscope (Nikon TE300 equipped with a 40x plan fluor objective, Crest V3 confocal imager and 89 North LDI-7 lasers) while incubated in 20 mM HEPES-containing complete DMEM, pH 7.4. This chamber is attached to a Peltier temperature regulating device (Warner Scientific) to keep the cell medium at ~ 37 ºC. BHQ-containing and BHQ-free buffered DMEM solutions were loaded in the perfusion system, which is also attached to a temperature-regulating device to keep delivered solutions at 37 ºC. BHQ was used at a concentration of 4 μM. Perfusion-controlling software was used to allow for exposure of cells to BHQ-free medium for 7 minutes, BHQ-containing medium for 3 minutes followed by perfusion with BHQ-free medium for up to 40 minutes. Images were collected every minute for chosen cells at multiple positions in the coverslip..

To analyze changes in intensities of the transfected proteins at ER exit sites, a uniform ROI was placed around the Halo-Sec31A labeled puncta in the perinuclear area (representing ER exit sites), and the mean intensity of the ROI was measured for every frame of the time-lapse image. The same ROI was used to measure the mean intensity for Sec13-GFP and mRuby2-ALG-2 in the same images. A total of 7 cells were analyzed. Individual cell intensities were graphed after normalizing the start of each trace to a value of 1.

## References


**1.** Alvarez J, Montero M. Measuring [Ca2+] in the endoplasmic reticulum with aequorin. Cell Calcium. 2002 Nov-Dec;32(5-6):251-60. https://doi.org/10.1016/s0143416002001860

**2.** Solovyova N, Verkhratsky A. Monitoring of free calcium in the neuronal endoplasmic reticulum: an overview of modern approaches. J Neurosci Methods. 2002 Dec 31;122(1):1-12. https://doi.org/10.1016/s0165-0270(02)00300-x

**3.** Clapham DE. Calcium signaling. Cell. 2007 Dec 14;131(6):1047-58. https://doi.org/10.1016/j.cell.2007.11.028

**4.** Michalak M, Robert Parker JM, Opas M. Ca2+ signaling and calcium binding chaperones of the endoplasmic reticulum. Cell Calcium. 2002 Nov-Dec;32(5-6):269-78. https://doi.org/10.1016/s0143416002001884

**5.** Wada I, Rindress D, Cameron PH, Ou WJ, Doherty JJ 2nd, Louvard D, Bell AW, Dignard D, Thomas DY, Bergeron JJ. SSR alpha and associated calnexin are major calcium binding proteins of the endoplasmic reticulum membrane. J Biol Chem. 1991 Oct 15;266(29):19599-610. https://doi.org/10.1016/S0021-9258(18)55036-5

**6.** Baksh S, Michalak M. Expression of calreticulin in Escherichia coli and identification of its Ca2+ binding domains. J Biol Chem. 1991 Nov 15;266(32):21458-65. https://doi.org/10.1016/S0021-9258(18)54661-5

**7.** Lièvremont JP, Rizzuto R, Hendershot L, Meldolesi J. BiP, a major chaperone protein of the endoplasmic reticulum lumen, plays a direct and important role in the storage of the rapidly exchanging pool of Ca2+. J Biol Chem. 1997 Dec 5;272(49):30873-9. https://doi.org/10.1074/jbc.272.49.30873

**8.** Sehgal P, Szalai P, Olesen C, Praetorius HA, Nissen P, Christensen SB, Engedal N, Møller JV. Inhibition of the sarco/endoplasmic reticulum (ER) Ca2+-ATPase by thapsigargin analogs induces cell death via ER Ca2+ depletion and the unfolded protein response. J Biol Chem. 2017 Dec 1;292(48):19656-19673. https://doi.org/10.1074/jbc.M117.796920

**9.** Xu, H., Van Remmen, H. The SarcoEndoplasmic Reticulum Calcium ATPase (SERCA) pump: a potential target for intervention in aging and skeletal muscle pathologies. Skeletal Muscle. 2021;11- 25. https://doi.org/10.1186/s13395-021-00280-7

**10.** Taylor CW, Tovey SC. IP(3) receptors: toward understanding their activation. Cold Spring Harb Perspect Biol. 2010 Dec;2(12):a004010. https://doi.org/10.1101/cshperspect.a004010

**11.** Kobayashi T, Kurebayashi N, Murayama T. The Ryanodine Receptor as a Sensor for Intracellular Environments in Muscles. Int J Mol Sci. 2021 Oct 6;22(19):10795. https://doi.org/10.3390/ijms221910795

**12.** Strehler EE. Plasma membrane calcium ATPases as novel candidates for therapeutic agent development. J Pharm Pharm Sci. 2013;16(2):190-206. https://doi.org/10.18433/j3z011

**13.** Gemmer M, Förster F. A clearer picture of the ER translocon complex. J Cell Sci. 2020 Feb 4;133(3):jcs231340. https://doi.org/10.1242/jcs.231340

**14.** Adams BM, Canniff NP, Guay KP, Hebert DN. The Role of Endoplasmic Reticulum Chaperones in Protein Folding and Quality Control. Prog Mol Subcell Biol. 2021;59:27-50. https://doi.org/10.1007/978-3-030-67696-4_3

**15.** Wang Q, Groenendyk J, Michalak M. Glycoprotein Quality Control and Endoplasmic Reticulum Stress. Molecules. 2015 Jul 28;20(8):13689-704. https://doi.org/10.3390/molecules200813689
**16.** Behnke J, Feige MJ, Hendershot LM. BiP and its nucleotide exchange factors Grp170 and Sil1: mechanisms of action and biological functions. J Mol Biol. 2015 Apr 10;427(7):1589-608. https://doi.org/10.1016/j.jmb.2015.02.011
**17.** Farhan H, Weiss M, Tani K, Kaufman RJ, Hauri HP. Adaptation of endoplasmic reticulum exit sites to acute and chronic increases in cargo load. EMBO J. 2008 Aug 6;27(15):2043-54. https://doi.org/10.1038/emboj.2008.136
**18.** Hasnain SZ, Prins JB, McGuckin MA. Oxidative and endoplasmic reticulum stress in β-cell dysfunction in diabetes. J Mol Endocrinol. 2016 Feb;56(2):R33-54. https://doi.org/10.1530/JME-15-0232
**19.** Oslowski CM, Urano F. Measuring ER stress and the unfolded protein response using mammalian tissue culture system. Methods Enzymol. 2011;490:71-92. https://doi.org/10.1016/B978-0-12-385114-7.00004-0
**20.** Preston AM, Gurisik E, Bartley C, Laybutt DR, Biden TJ. Reduced endoplasmic reticulum (ER)-to-Golgi protein trafficking contributes to ER stress in lipotoxic mouse beta cells by promoting protein overload. Diabetologia. 2009 Nov;52(11):2369-2373. https://doi.org/10.1007/s00125-009-1506-5
**21.** Shaheen A. Effect of the unfolded protein response on ER protein export: a potential new mechanism to relieve ER stress. Cell Stress Chaperones. 2018 Sep;23(5):797-806. https://doi.org/10.1007/s12192-018-0905-2
**22.** Bartoszewska S, Collawn JF. Unfolded protein response (UPR) integrated signaling networks determine cell fate during hypoxia. Cell Mol Biol Lett. 2020 Mar 13;25:18. https://doi.org/10.1186/s11658-020-00212-1
**23.** D'Arcangelo JG, Stahmer KR, Miller EA. Vesicle-mediated export from the ER: COPII coat function and regulation. Biochim Biophys Acta. 2013 Nov;1833(11):2464-72. https://doi.org/10.1016/j.bbamcr.2013.02.003
**24.** Trahey M, Hay JC. Transport vesicle uncoating: it's later than you think. F1000 Biol Rep. 2010;2:47. https://doi.org/10.3410/b2-47
**25.** Maki M, Yamaguchi K, Kitaura Y, Satoh H, Hitomi K. Calcium-induced exposure of a hydrophobic surface of mouse ALG-2, which is a member of the penta-EF-hand protein family. J Biochem. 1998 Dec 1;124(6):1170-7. https://doi.org/10.1093/oxfordjournals.jbchem.a022235
**26.** Lo KW, Zhang Q, Li M, Zhang M. Apoptosis-linked gene product ALG-2 is a new member of the calpain small subunit subfamily of Ca2+-binding proteins. Biochemistry. 1999 Jun 8;38(23):7498-508. https://doi.org/10.1021/bi990034n
**27.** Yamasaki A, Tani K, Yamamoto A, Kitamura N, Komada M. The Ca2+-binding protein ALG-2 is recruited to endoplasmic reticulum exit sites by Sec31A and stabilizes the localization of Sec31A. Mol Biol Cell. 2006 Nov;17(11):4876-87. https://doi.org/10.1091/mbc.e06-05-0444
**28.** Shibata H, Suzuki H, Yoshida H, Maki M. ALG-2 directly binds Sec31A and localizes at endoplasmic reticulum exit sites in a Ca2+-dependent manner. Biochem Biophys Res Commun. 2007 Feb 16;353(3):756-63. https://doi.org/10.1016/j.bbrc.2006.12.101
**29.** la Cour JM, Schindler AJ, Berchtold MW, Schekman R. ALG-2 attenuates COPII budding in vitro and stabilizes the Sec23/Sec31A complex. PLoS One. 2013 Sep 19;8(9):e75309. https://doi.org/10.1371/journal.pone.0075309
**30.** Kitaura Y, Watanabe M, Satoh H, Kawai T, Hitomi K, Maki M. Peflin, a novel member of the five-EF-hand-protein family, is similar to the apoptosis-linked gene 2

(ALG-2) protein but possesses nonapeptide repeats in the N-terminal hydrophobic region. Biochem Biophys Res Commun. 1999 Sep 16;263(1):68-75. https://doi.org/10.1006/bbrc.1999.1189
**31.** Kitaura Y, Matsumoto S, Satoh H, Hitomi K, Maki M. Peflin and ALG-2, members of the penta-EF-hand protein family, form a heterodimer that dissociates in a Ca2+-dependent manner. J Biol Chem. 2001 Apr 27;276(17):14053-8. https://doi.org/10.1074/jbc.M008649200
**32.** Kitaura Y, Satoh H, Takahashi H, Shibata H, Maki M. Both ALG-2 and peflin, penta-EF-hand (PEF) proteins, are stabilized by dimerization through their fifth EF-hand regions. Arch Biochem Biophys. 2002 Mar 1;399(1):12-8. https://doi.org/10.1006/abbi.2001.2736
**33.** Gustavsson N, Wu B, Han W. Calcium sensing in exocytosis. Adv Exp Med Biol. 2012;740:731-57. https://doi.org/10.1007/978-94-007-2888-2_32
**34.** Micaroni M, Perinetti G, Berrie CP, Mironov AA. The SPCA1 Ca2+ pump and intracellular membrane trafficking. Traffic. 2010 Oct;11(10):1315-33. https://doi.org/10.1111/j.1600-0854.2010.01096.x Erratum in: Traffic. 2011 Jun;12(6):789. Mironov, Alexander A
**35.** Micaroni M. Calcium around the Golgi apparatus: implications for intracellular membrane trafficking. Adv Exp Med Biol. 2012;740:439-60. https://doi.org/10.1007/978-94-007-2888-2_18
**36.** Beckers CJ, Balch WE. Calcium and GTP: essential components in vesicular trafficking between the endoplasmic reticulum and Golgi apparatus. J Cell Biol. 1989 Apr;108(4):1245-56. https://doi.org/10.1083/jcb.108.4.1245
**37.** Helm JR, Bentley M, Thorsen KD, Wang T, Foltz L, Oorschot V, Klumperman J, Hay JC. Apoptosis-linked gene-2 (ALG-2)/Sec31 interactions regulate endoplasmic reticulum (ER)-to-Golgi transport: a potential effector pathway for luminal calcium. J Biol Chem. 2014 Aug 22;289(34):23609-28. https://doi.org/10.1074/jbc.M114.561829
**38.** Rayl M, Truitt M, Held A, Sargeant J, Thorsen K, Hay JC. Penta-EF-Hand Protein Peflin Is a Negative Regulator of ER-To-Golgi Transport. PLoS One. 2016 Jun 8;11(6):e0157227. https://doi.org/10.1371/journal.pone.0157227
**39.** Sargeant J, Seiler DK, Costain T, Madreiter-Sokolowski CT, Gordon DE, Peden AA, Malli R, Graier WF, Hay JC. ALG-2 and peflin regulate COPII targeting and secretion in response to calcium signaling. J Biol Chem. 2021 Dec;297(6):101393. https://doi.org/10.1016/j.jbc.2021.101393
**40.** Rivera VM, Wang X, Wardwell S, Courage NL, Volchuk A, Keenan T, Holt DA, Gilman M, Orci L, Cerasoli F Jr, Rothman JE, Clackson T. Regulation of protein secretion through controlled aggregation in the endoplasmic reticulum. Science. 2000 Feb 4;287(5454):826-30. https://doi.org/10.1126/science.287.5454.826
**41.** Mezzacasa A, Helenius A. The transitional ER defines a boundary for quality control in the secretion of tsO45 VSV glycoprotein. Traffic. 2002 Nov;3(11):833-49. https://doi.org/10.1034/j.1600-0854.2002.31108.x
**42.** Pontén J, Saksela E. Two established in vitro cell lines from human mesenchymal tumours. Int J Cancer. 1967 Sep 15;2(5):434-47. https://doi.org/10.1002/ijc.2910020505
**43.** McGourty CA, Akopian D, Walsh C, Gorur A, Werner A, Schekman R, Bautista D, Rape M. Regulation of the CUL3 Ubiquitin Ligase by a Calcium-Dependent Co-adaptor. Cell. 2016 Oct 6;167(2):525-538.e14. https://doi.org/10.1016/j.cell.2016.09.026

**44.** Pang ZP, Südhof TC. Cell biology of Ca2+-triggered exocytosis. Curr Opin Cell Biol. 2010 Aug;22(4):496-505. https://doi.org/10.1016/j.ceb.2010.05.001
**45.** Fu Z, Gilbert ER, Liu D. Regulation of insulin synthesis and secretion and pancreatic Beta-cell dysfunction in diabetes. Curr Diabetes Rev. 2013 Jan 1;9(1):25-53. http://dx.doi.org/10.2174/1573399811309010025
**46.** Poitout V, Hagman D, Stein R, Artner I, Robertson RP, Harmon JS. Regulation of the insulin gene by glucose and fatty acids. J Nutr. 2006 Apr;136(4):873-6. https://doi.org/10.1093/jn/136.4.873
**47.** Akopian D, McGourty CA, Rapé M. Co-adaptor driven assembly of a CUL3 E3 ligase complex. Mol Cell. 2022 Feb 3;82(3):585-597.e11. https://doi.org/10.1016/j.molcel.2022.01.004
**48.** Jin L, Pahuja KB, Wickliffe KE, Gorur A, Baumgärtel C, Schekman R, Rape M. Ubiquitin-dependent regulation of COPII coat size and function. Nature. 2012 Feb 22;482(7386):495-500. https://doi.org/10.1038/nature10822
**49.** Moretti T, Kim K, Tuladhar A, Kim J. KLHL12 can form large COPII structures in the absence of CUL3 neddylation. Mol Biol Cell. 2023 Mar 1;34(3):br4. https://doi.org/10.1091/mbc.E22-08-0383
**50.** Hammond AT, Glick BS. Dynamics of transitional endoplasmic reticulum sites in vertebrate cells. Mol Biol Cell. 2000 Sep;11(9):3013-30. https://doi.org/10.1091/mbc.11.9.3013
**51.** Weigel AV, Chang CL, Shtengel G, Xu CS, Hoffman DP, Freeman M, Iyer N, Aaron J, Khuon S, Bogovic J, Qiu W, Hess HF, Lippincott-Schwartz J. ER-to-Golgi protein delivery through an interwoven, tubular network extending from ER. Cell. 2021 Apr 29;184(9):2412-2429.e16. https://doi.org/10.1016/j.cell.2021.03.035